Real time plasma etch control by means of physical plasma parameters with SEERS

Andreas Steinbach[a], Martin Sussiek[d], Siegfried Bernhard[a], Stefan Wurm[b], Christian Koelbl[c], Daniel Köhler[a]

[a]Siemens Microelectronics Center, Dresden, Germany
[b]Siemens at International Sematech, Austin, TX
[c]Siemens Regensburg, Germany
[d]Technische Universität Hamburg – Harburg, Germany

The European Symposium on Microelectronic Manufacturing Technologies
19-21 May 1999
Caledonian Hotel, Edinburgh, Scotland, United Kingdom

Real time plasma etch control by means of physical plasma parameters with SEERS

Andreas Steinbach[a], Martin Sussiek[d], Siegfried Bernhard[a],
Stefan Wurm[b], Christian Koelbl[c], Daniel Köhler[a], Dirk Knobloch[a]

[a]Siemens Microelectronics Center, Dresden, Germany
[b]Siemens at International Sematech, Austin, TX
[c]Siemens Regensburg, Germany
[d]Universität Hamburg – Harburg, Germany

ABSTRACT

The plasma monitoring system HERCULES utilizes the Self Excited Electron Plasma Resonance Spectroscopy (SEERS) technique. It takes into account the non-linearity of the space charge sheath at the rf electrode, which provides harmonics with the modulated sheath width and high frequency oscillations in the bulk plasma. By using a general discharge model, SEERS provides volume averaged values of electron collision rate, electron density, and bulk power. It thus provides a very efficient real time data compression. The rf sensor head at the chamber wall is on ground potential and does not influence plasma- or process conditions. The sensor measures rf currents only, hence, there is no impact of polymer or other insulating layers on the measured signals. HERCULES is the first process control tool providing real-time accessibility to plasma parameters - based on an electrical measurement principle - for rf plasmas under industrial conditions.
The efficient data handling being ready for use in production includes an internal process data bank and offers two ways to control the process: 1.) independent of the etch tool, and 2.) using a data coupling utility providing fast and easy access to wafer and lot data. Here, the second possibility was used based on a chamber log-sheet for lot and single wafer control. The major benefit of this choice is that data can be analyzed by lot and product using standard software.
The SEERS tool demonstrated a high sensitivity and significant correlation of measured signals to variations of fundamental process parameters. It was found to be well suited to control stability of process equipment and to support process optimization and development. Important suppliers, e.g. Applied Materials and Lam Research, have supported the assessment and are interested in applying this process control tool.

Keywords: Oxide etching, Al etching, SEERS, process monitoring, plasma sensor, HERCULES, real time, non-productive wafer reduction, plasma diagnostics

1. INTRODUCTION

Semiconductor technology is one of the major applications of low temperature plasmas. Today, semiconductor production is characterized by ever-faster changes to higher integration levels. Feature sizes with critical dimensions of 0.2 µm to 0.17 µm are used in high volume production already, and structures of 0.15 µm to 0.12 µm are targeted for the next shrink steps. Parallel to this technology shrink, the semiconductor industry switches over to a larger wafer diameter. Current Si wafers usually have a diameter of 200 mm. However, the first European 300 mm semiconductor fab, a joint venture of Siemens and Motorola in Dresden, has already started production.
All these efforts are made to enable cost effective production of semiconductor devices with higher complexity. In memory production 64 M DRAM´s are produced in high volume now. The production of 256 M DRAM´s has been started already and 1 G DRAM´s are expected within the next two years.
In contrast to this fast development of integration level and wafer size, production strategy is developing slowly. For process development, experience and statistical methods are mainly used. With only few exceptions, tools are still monitored and/or controlled using many costly test wafers, i.e. non-productive wafers, and time consuming procedures, i.e. non-available process time. For control of process results additional in – line measurements are necessary. Statistical Process Control is widely used. Tool- and wafer costs are increasing rapidly, therefore, the established methods of process development, tool control, and process control become more and more expensive and ineffective.
In – situ measurement techniques for real time process monitoring on product wafers can provide unique possibilities to reduce the number of non - productive wafers, to increase tool up - time, and to improve process

stability. Most likely, those techniques will be indispensable to reduce production costs and improve profitability [1, 2].
Though plasma etch is a key process in semiconductor manufacturing technology, in – situ process controls for plasma etching are still very poorly developed. The plasma monitoring system HERCULES is one example for the new in – situ real time measuring techniques, which are ready for use in semiconductor production.

2. WHY IS REAL TIME PLASMA MONITORING NECESSARY

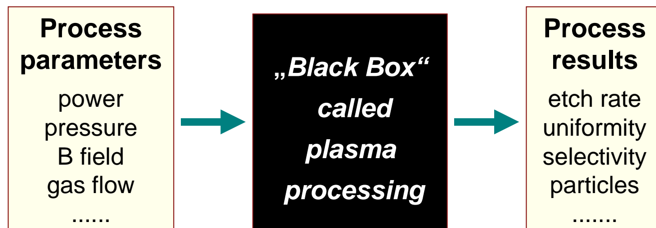

Figure 1: Industrial plasma processing today

Plasma processes as used in semiconductor manufacturing are usually treated as “black boxes” (see Figure 1). Process parameters, e.g., power output of the rf generator, discharge pressure, B – field, and gas flows, are measured at the tool. Etch results are measured on test or product wafers. This is done in order to maintain constant process conditions and to achieve the same etch results on all product wafers.
But, in fact, these “process” parameters, are more related to tool parameters and not to real process parameters. In addition, these measurements can have significant errors or provide only a small amount of relevant information. RF power measurement can serve as a typical example. RF power is measured at the output of the rf generator. There are power losses on the cable between the generator output and the RF matchbox input, inside the match box, and at the connector from the output of the match to the wafer electrode in the chamber. These power losses are unknown and they vary from tool to tool and from process to process. But even if we could guarantee a constant power input into the chamber, the rf power is not a true measure for well known process conditions, due to, e.g., secondary plasmas and changing chamber conditions like polymer build-up on the chamber walls.
Etch rates, uniformity’s, and particle densities are usually measured on blank test wafers. Even if the tool parameters are the same, etch chemistries in the plasma are certainly different for blank oxide test wafers and product wafers, with the latter being covered with a photo resist mask. Test wafers are often less sensitive to changes of process conditions than product wafers. That is why test results can be constant, while the product yield decreases.
Experience and statistical methods, e.g., design of experiment, are used to develop and optimize processes. Processes can not be directly transferred between tools since the real important process parameters in the plasma are not known. More realistically, process transfer quite often is synonymous to new process development.

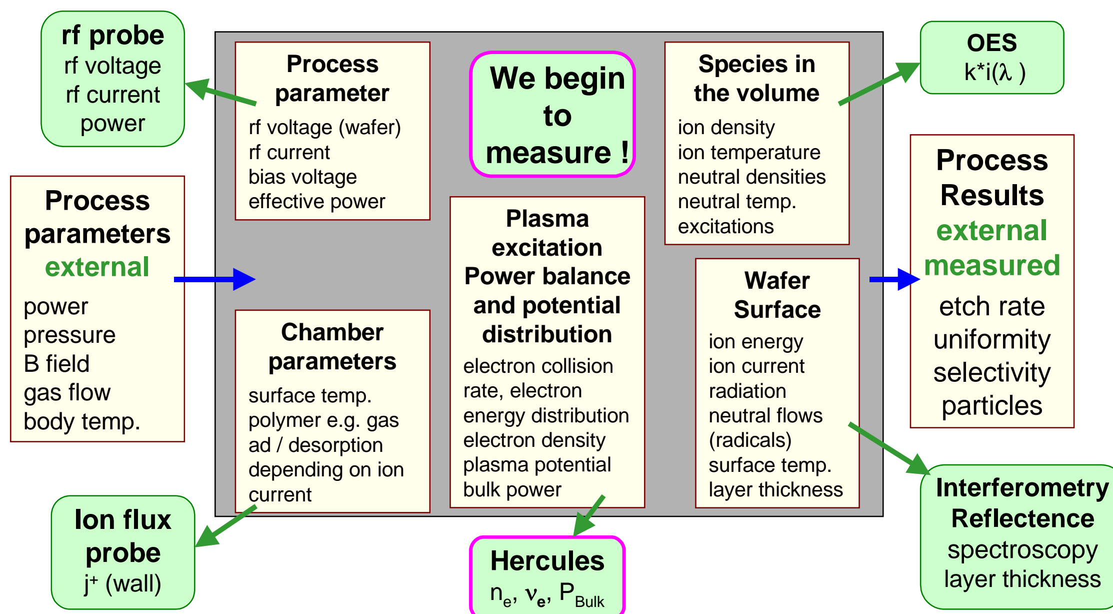

Figure 2: Measuring techniques for in – situ real time plasma monitoring [3, 4, 5, 6]

If we look into the “black box”, shown in Figure 2, we find many interacting phenomena [3, 4, 5, 6]. Plasma excitation, power balance, and potential distribution depend on external process parameters, which are measured at industrial tools, and on other process parameters, e.g., rf voltage, rf current, bias voltage, and effective power, which are usually not measured [16]. Plasma excitation and process parameters impact the species in the discharge volume. However, of decisive importance for the etching result are the conditions on the wafer surface. They depend very much on the plasma excitation and the species in the volume. To some extent, unknown chamber parameters, such as surface temperature, adsorption and desorption of process gases, and gaseous etch products in polymer layers on the chamber wall, have a strong impact as well.
Constant etch results can only be obtained by stable conditions at the wafer surface. To achieve this goal is a tricky thing. Therefore several measurement techniques have been developed to measure at “different corners” of the “black box”. Optical methods are well known, e.g. for endpoint detection. One of the new electrical methods is **S**elf **E**xcited **E**lectron plasma **R**esonance **S**pectroscopy (SEERS) as implemented by the plasma monitoring system HERCULES [11,12,13,14,15]. It can measure important plasma parameters, such as electron collision rate, electron density, and bulk power. Therefore, this technique can be expected to provide information about reactions on the wafer surface and about tool conditions [3,4,5,6,7, 8].

3. THEORETICAL BACKGROUND AND EXPERIMENTAL SETUP

The **S**elf **E**xcited **E**lectron plasma **R**esonance **S**pectroscopy (SEERS) is based on the non-linearity of the space charge sheath at the rf electrode, which provides harmonics with the modulated sheath width and high-frequency oscillations in the plasma bulk [9, 10, 11, 12, 13, 14, 15].

$$\frac{du}{dt} = \frac{s[u(t)]\, i(t)}{A_0\, \epsilon_0} \qquad (1)$$

In order to include the non-linear sheath capacitance, the fundamental relation between temporal derivative of sheath voltage u, sheath width s[u] and displacement current i [10]:
is used, which indicates the nonlinear properties of the sheath. A_0 denotes the rf electrode area. The degree of the nonlinearity depends on the ion density distribution within the sheath and results basically in a saw tooth shaped current.
Using a hydrodynamic approach for the electrons, the known equation for the permittivity of the cold plasma can be expressed as [14].

$$\frac{\epsilon}{\epsilon_0} = 1 - \frac{\omega_e^2}{\omega(\omega - \mathrm{j}\,\nu)} \;,\quad \omega_e^2 = 1 - \frac{e^2 n}{\epsilon_0\, m_e} \qquad (2)$$

where ω_e is the electron plasma (Langmuir) frequency. When the collision rate ν vanishes, Eq. (2) is known as Eccles relation.
Bearing in mind the relation between electrostatic field and current density $J = \mathrm{j}\omega\varepsilon E$ for $(\omega_e/\omega)^2 >> 1+(\nu/\omega)^2$, the conductivity can be written as [14]

$$\sigma_p = \frac{n\, e^2}{m_e\, (\mathrm{j}\omega + \nu)} \;, \qquad (3)$$

and the potential drop of the bulk plasma in the time domain as

$$u_p = \frac{m_e l}{A_0\, n\, e^2} \left(\nu\, i + \frac{d}{dt}\, i \right) \;. \qquad (4)$$

The effective length of the plasma body is obtained by a two - dimensional treatment of rf current distribution at given boundary conditions. Neglecting the conduction currents of ions and electrons in the sheath, however, one obtains

$$\frac{d}{dt} u_{rf} + \frac{\bar{s} - s[u(t)]}{A_0\, \epsilon_0} i = \frac{\bar{s}}{A_0\, \epsilon_0} i + \frac{m_e l}{A_0\, n\, e^2} \left(\nu i + \frac{d}{dt} i + \frac{d^2}{dt^2} i \right) \quad (5)$$

for the whole discharge driven by the voltage u_{rf} at the rf electrode (see Figure 3) [14].
This is a non-linear, inhomogeneous, and stiff differential equation of second order. On the right hand side of the equation above is a linear oscillation term with the geometric resonance frequency $\omega_p^2 = \omega_e^2\, s/l$ for a plasma with small damping, where l denotes the effective geometric length of the plasma.
The dependence of the sheath width on the displacement current involves a special approach and usually requires a numerical solution of the differential equation (5).
This differential equation can be interpreted using an equivalent circuit (compare Figure 3). On the left-hand side, we have the external excitation - the matchbox including the rf generator. The discharge is treated as a damped oscillating circuit as suggested by the right hand side of Eq. (5).
Finally we have the non-linear phenomena, given by the second term on the left-hand side of Eq. (5). The non-linearity of the sheath, compare with Eq. (1), provides harmonics exciting the oscillating circuit. This additional resonance can be observed by measuring the discharge current. SEERS allows the determination of the volume averaged electron density,

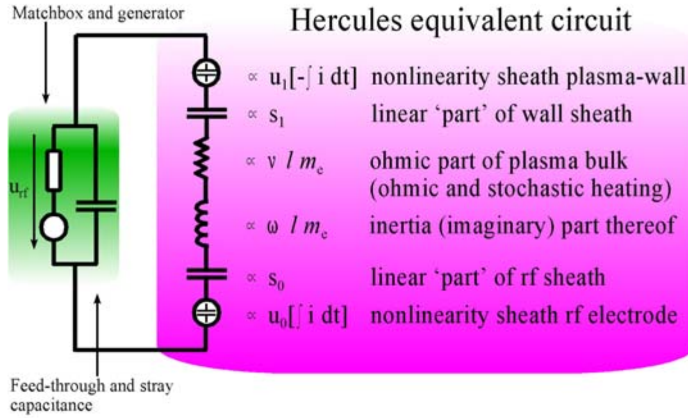

Figure 3: Equivalent circuit of radio frequency discharge

$$\tilde{n} = \frac{1}{V} \left(\int_V n^{-1}\, dV \right) \quad (6)$$

electron collision rate [14,17],

$$\tilde{\nu} = \frac{\tilde{n}}{V} \left(\int_V \frac{\nu}{n}\, dV \right) \quad (7)$$

and bulk power dissipated in the plasma body:

$$P_B = \frac{\tilde{\nu}}{\tilde{n}} \sum_{(k)} \left[I(k) \right]^2 \quad (8)$$

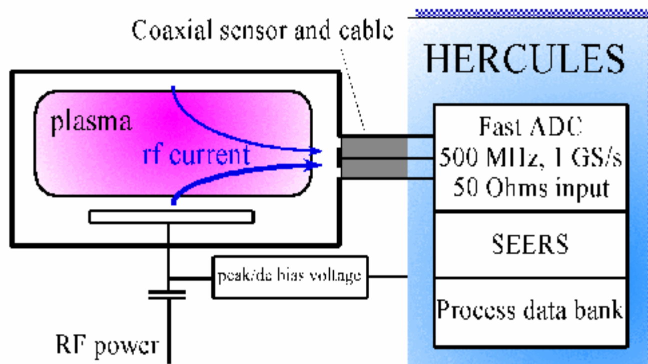

Figure 4: Experimental setup

Using a fast numerical algorithm, the plasma monitoring system HERCULES provides a temporal resolution better than a second and performs SEERS measurements automatically.
The experimental setup and some sensor types are shown in Figure 4 and Figure 5. Because of unavoidable stray and feedthrough capacitances at the powered electrode, a direct measurement of the discharge current is very difficult in commercial systems. HERCULES uses a special sensor in a coaxial geometry (50 Ω) inserted into the wall (flange) of the recipient as a virtual part of the wall. By means of the nonlinear model, the current pitch ratio of the current measured and the real discharge current can

be determined. Therefore, calibration depending on the sensor position is not necessary. An insulating layer up to a thickness of 100 µm on the sensor can be treated as a capacitance adding a very small series impedance (<< 50 Ω) and can be therefore neglected. The measured discharge current is converted using a fast ADC (analog / digital converter) with a bandwidth of 500 MHz and a sampling rate of 2 GS/s.

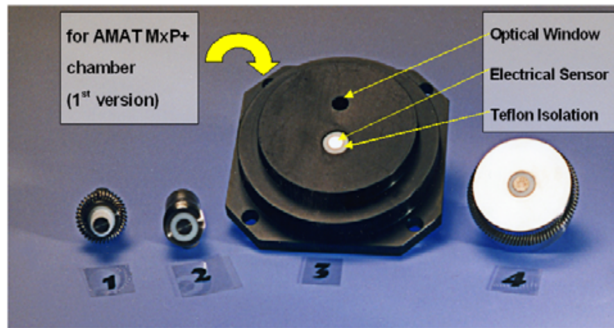

Figure 5: HERCULES sensor types

The peak voltage of the substrate is measured by using a capacitive voltage divider. At many industrial tools the peak voltage and even the bias voltage are not available. In this case, the sheath thickness is estimated to be constant. As a result of this simple approximation, electron density, bulk power, and the calculated bias voltage have a systematic deviation.

Many plasma processes use a rotating magnetic field. Here the measurement is triggered by a Hall sensor. In a process data base, the process data are stored together with logistical data, e.g. date, time, chamber, lot name, and recipe step. The size of a data file for one lot (25 wafers) is about 100 kB. In comparison to other methods, these files are small and easy to handle.

4. BASIC EXPERIMENTS

4.1. Sensitivity to process parameter variations at oxide etch in Applied Materials MxP+ chamber

Basic experiments were done using a CF_4, CHF_3, Ar gas mixture for oxide etch at an Applied Materials MxP+ chamber, with blank doped oxide wafers (BPSG) and patterned test wafers for contact etch. Typical examples of the results are shown in Figure 6 and Figure 7.

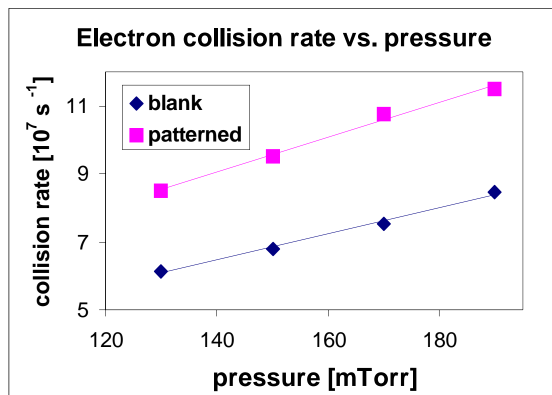

Figure 6: Electron collision rate depending on pressure at Oxide etch in AMAT MxP+ chamber

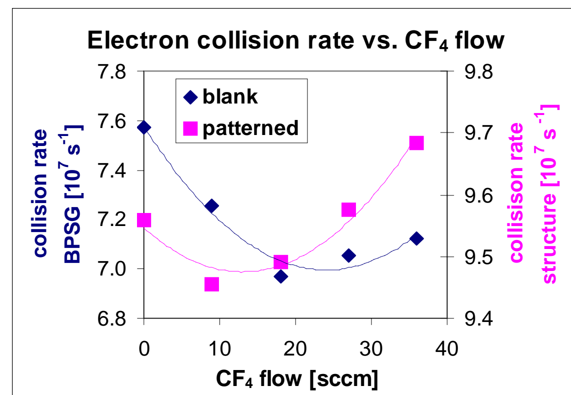

Figure 7: Electron collision rate depending on and CF_4 flow at Oxide etch in AMAT MxP+ chamber

Variations of "physical" process parameters, e.g., rf power or pressure cause partly nonlinear correlation between measured plasma parameters and process parameters (however, quite often a monotonous or quasi linear dependence has been found). Variations of the "plasma chemistry", e.g., of the CF_4 or O_2 flow, result in often strong nonlinear effects. Electron collision rate, electron density, and bulk power depend significantly on all process parameter changes and on the wafer surface.

4.2. Correlation between plasma parameters and etch results on test wafers

For industrial applications it would be very desirable, to be able to characterize and classify etch rate results by using only measured plasma parameters. The following examples demonstrate that this can be achieved (see Figure 8 and Figure 9).

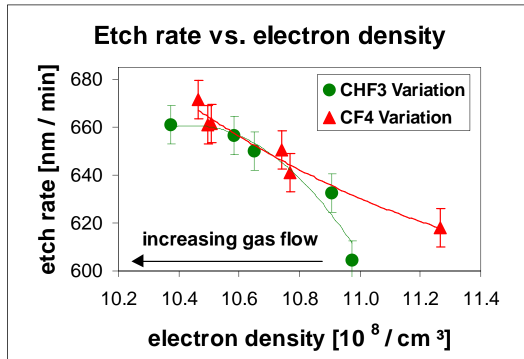

Figure 8: Correlation between BPSG etch rate and electron density

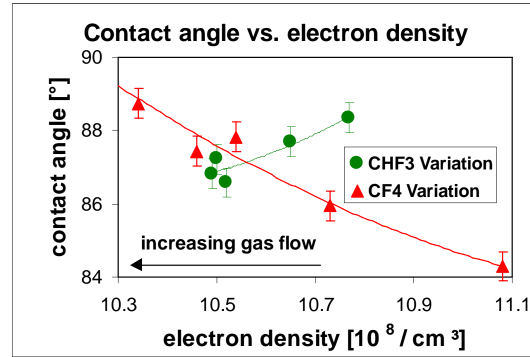

Figure 9: Correlation between contact hole angle and electron density

In a typical oxide or nitride etch gas mixture consisting of CF_4, CHF_3, Ar, and O_2, an increasing CF_4 - or CHF_3 -flow causes a lower electron density. These two reactive gases, however, effect discharge chemistry in completely different ways. CF_4 delivers particularly CF_2- and F radicals and ions. On the contrary, the main fragments of CHF_3 dissociation are CHF_x components driving polymerization. Therefore, increasing the gas flow for CHF_3 or CF_4 results in higher BPSG etch rates, whereas the way the two gases effect the contact hole etch are very different. A higher CHF_3 –flow increases the polymerization, gives a better side wall passivation and a lower contact angle. A higher CF_4 – flow creates a higher concentration of F etch species and therefore a steeper contact angle. Due to the oxide etch chemistry, a one-to-one correlation between electron density and contact angle is not possible. Generally, a change of the electron density or any other measured parameter indicates a variation of the discharge conditions.

5. PROCESS AND TOOL STABILITY

5.1. Long term process stability

A mixture of oxide and nitride etch processes has been monitored at an Applied Materials MxP+ chamber for more than 450 rf hours to characterise the long term stability of these processes. Figure 10 shows the trend of the electron collision rate for oxide etch during 5 wet clean cycles (WC). During WC1 and WC3 a continuos shift was observed, while the electron collision rate was comparatively constant during WC2, WC4, and WC5, however, on different levels.

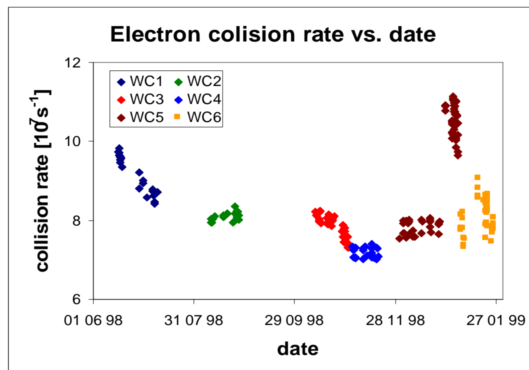

Figure 10: Dependence of electron collision rate on date of oxide etch process 1 (Pr1) during 6 wet clean cycles (WC); one point one lot.

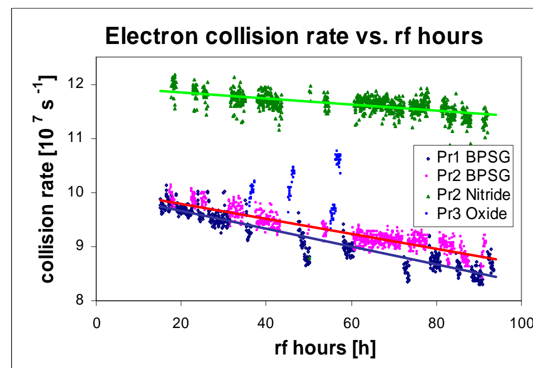

Figure 11: Electron collision rate as observed for oxide- and nitride etch used in three different processes at WC1; one point one wafer.

To make the wet clean as fast as possible, the MxP+ chamber is covered by removable liner parts inside. During the wet clean, all liner parts are changed for external cleaning. It seems, that the long term process stability depends on the wet clean, including the kind of liner set, reassembled in the chamber. Different spare part sets were used, new ones, regenerated ones, and already many times used ones. The reason for the differences detected could not be traced back in detail, because the spare parts were not tracked individually. Therefore, as of yet, no correlation could be done between measurements and hardware used inside the chamber.

Figure 11 compares electron collision rates of oxide etch processes using a one-step recipe (Pr1), a three-step recipe (Pr2) where the first process step is the same as for Pr1, and another oxide etch process (Pr3). All processes were executed during WC1. The two additional steps of Pr2 use different gas mixtures and cause a de-conditioning of the polymer at the chamber wall. Therefore, the difference of the electron collision rates of Pr1 and Pr2 increases with process time and, respectively, with the polymer thickness at the chamber wall. Hence, the electron collision rate can be used to control the polymer thickness. The values of the collision rate, observed for a nitride etch and the other oxide etch process (Pr3) are very different, according to their different discharge chemistry. Hence, electron collision rate is very sensitive to variations of the plasma chemistry.

5.2. First wafer effects and short term process stability

First wafer effects were detected at the LAM TCP during the main etch step of the first wafer (Al etch, see Figure 12), for which the electron density was significantly higher as compared to the next wafers [5]. This is connected with a higher etch time and therefore with a lower etch rate.

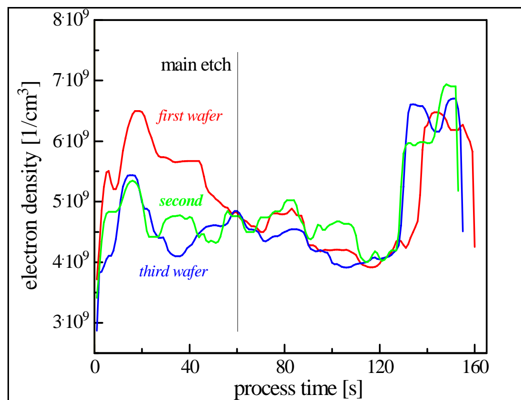

Figure 12: First wafer effect during Al etch at LAM TCP; one curve - one wafer

Depending on idle time, for the Applied Materials MxP+ chamber the electron collision rate was found to drift even after the first ten wafers had been etched (compare Figure 13). The drift effect increases with the idle time before processing the lot. This can be explained by a temperature drift of the liner cylinder and gas adsorption effects at the polymer layers inside the chamber.

Figure 14 shows an example of the technological relevance of such chamber drift effects in critical situations. Normally, such small chamber drifts can be neglected, if the process window is well designed. However, during an instable process integration period, this small chamber drift of about 2,5 % for contact etch caused higher electrical failure counts and therefore a lower yield. Hence, this comparison demonstrates that the values of plasma excitation parameters, as measured by HERCULES, are very sensitive and can provide critical leverage for controlling yield.

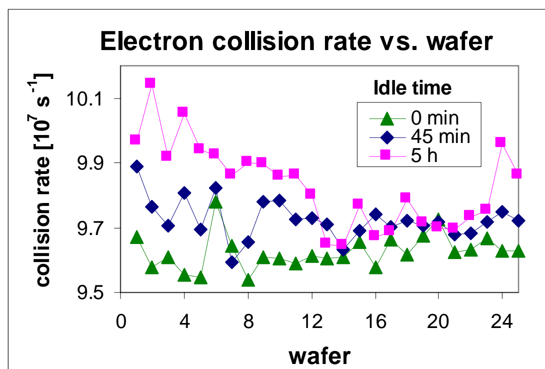

Figure 13: First wafer effect at oxide etch in MxP+; one point - one wafer

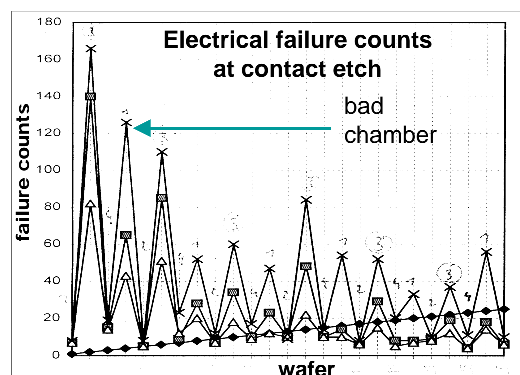

Figure 14: Electrical failure counts at contact etch show first wafer effect; one point - one wafer

5.3. Wafer effects

During long term process monitoring of oxide etch, lot depending process variations were found (see Figure 15). The lot means of the electron density shows two distinguishable levels. Two products were etched at this time with the same recipe. These two products differ in open area (i.e., ratio between the area of oxide and the area, covered with resist mask). As a result, the gas mixtures and therefore the electron densities are different. Other detected wafer effects could not be explained in detail yet.

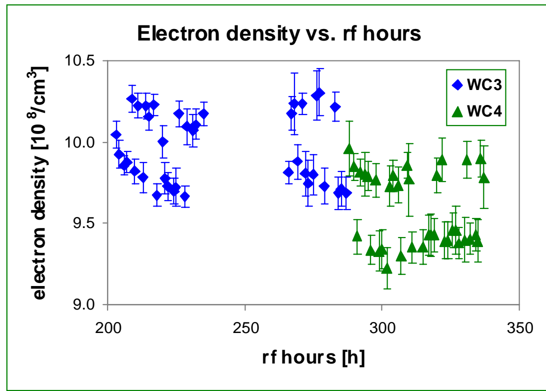

Figure 15: Wafer effect at oxide etch; one point - one lot mean

The following examples show HERCULES parameter being used to search for process problems in detail, while the system is running in automatic mode. Figure 16 and Figure 17 compare the values of electron collision rate and electron density, measured with a delay of about 6 weeks. While in July 98 the process was very stable, about 6 weeks later short term drifts and wafer effects were detected. Details of electron collision rate and electron density are shown in Figure 18 and Figure 19.

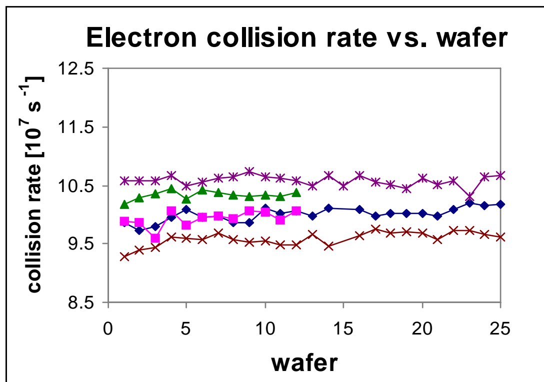

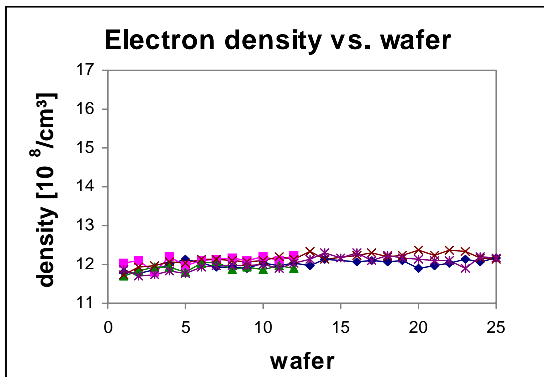

Figure 16: Early July 98: Electron collision rate and electron density of oxide etch; one point – one wafer

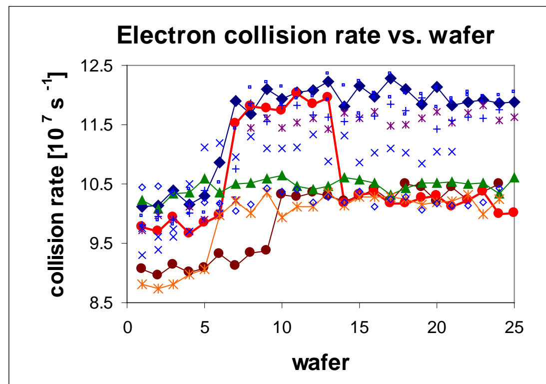

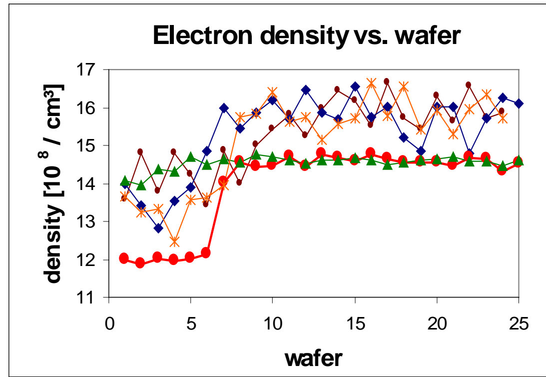

Figure 17: Late August 98: Electron collision rate and electron density of oxide etch; one point – one wafer

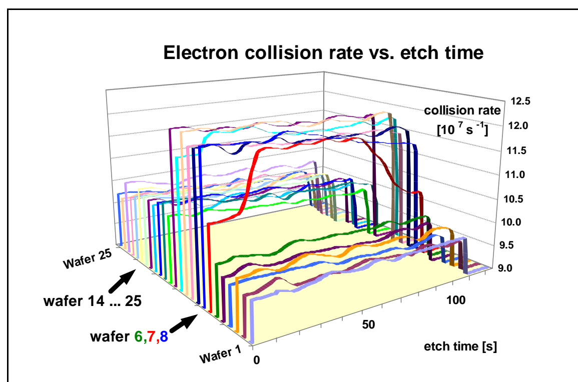

Figure 18: Time resolved curves of electron collision rate; one curve – one wafer

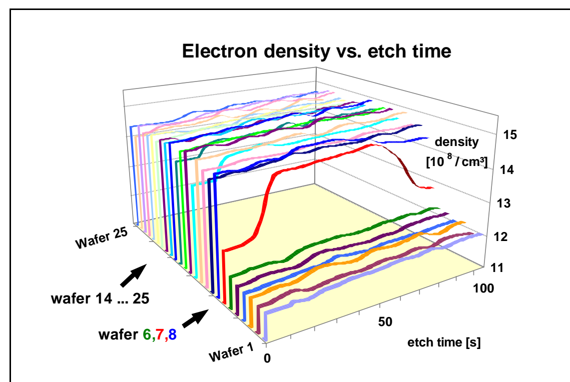

Figure 19: Time resolved curves of electron density; one curve – one wafer

In Figure 20 and Figure 21 electron collision rate and electron density are compared with the optical intensities of the CO – and the CN emission line as measured with the Applied Materials HOT Pack (optical endpoint system). The intensity of the CN emission line shows similar intensity variations.

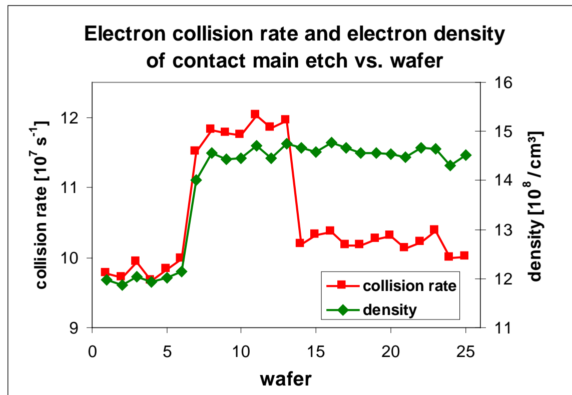

Figure 20: Wafer depending process variation for oxide etch of one lot, one point one wafer.

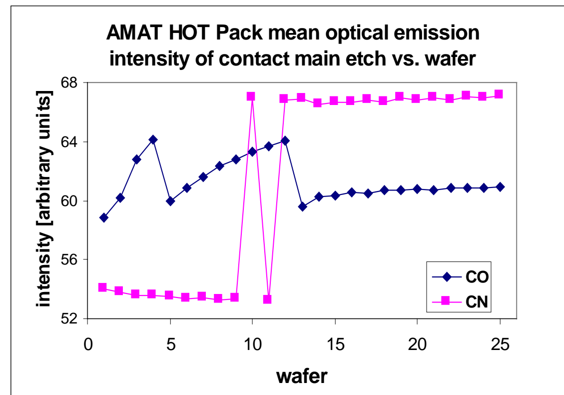

Figure 21: Wafer depending process instability for oxide etch of one lot, one point one wafer.

5.4 Endpoint detection

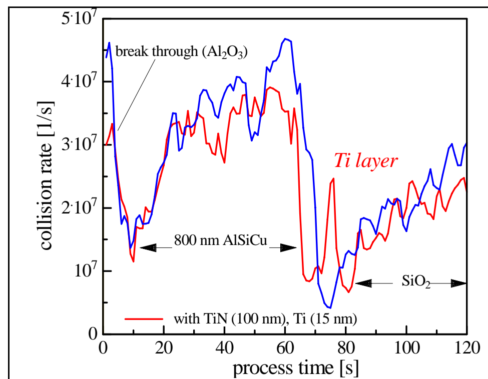

Figure 22: Endpoint detection during Al etch at LAM TCP

Figure 22 shows an example for endpoint detection at LAM TCP 9600SE [7, 8]. The Al etch process consists of three steps, the break-through, the main etch, and the over etch. Below the Al layer there is a stack of Ti and TiN. During the Al etch process at the LAM TCP after an etch time of about 75 s, a peak in collision rate appeared if the stack contained a Ti layer. By using a set of special test wafers, it could be verified that this peak is due to a 15 nm thick Ti layer. Very likely the large electron scattering cross section of Ti is the main reason for this effect. Therefore, HERCULES can be used for endpoint detection as well. For contact etch processes it was less sensitive than optical systems. In case of comparatively large open area and processes with a strong polymerization, this endpoint detection method can be more successful than optical ones.

5.5. Optimization of conditioning procedures

The impact of a wet clean on electron collision rate and electron density is shown in Figure 23 and Figure 24.

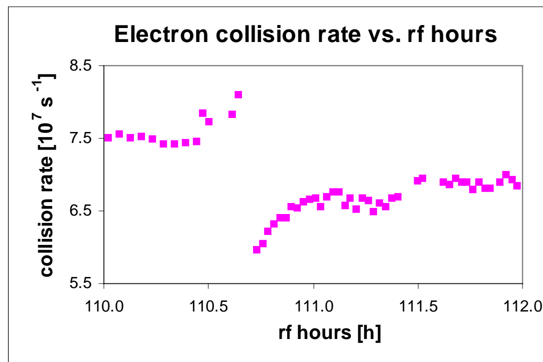

Figure 23: Electron collision rate before and after wet clean. Oxide etch, MxP+ chamber, one point - one wafer.

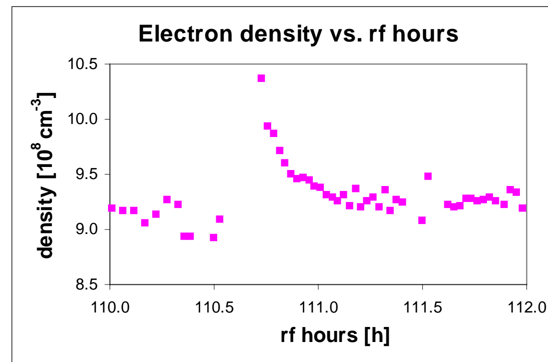

Figure 24: Electron density before and after wet clean. Oxide etch MxP+ chamber, one point - one wafer.

After the wet clean at 110.7 rf hours, resist wafers were used for chamber conditioning. Using this etch process, about 10 wafers are necessary to reach stabile process conditions after the wet clean. Obviously, the plasma monitoring system HERCULES can be used to optimize conditioning procedures and to reduce costs by saving resist wafers.

5.6. Power density measurement

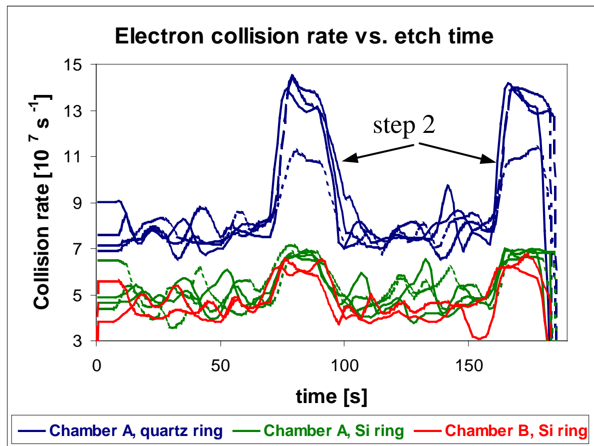

Figure 25: Power dissipation in a MxP chamber as monitored for a two step shows strong dependence on shadow ring permittivity.

Parameter	Ratio Si ring / Quartz ring
Nitride etch rate	**0.66**
Wafer temp.	**0.71**
Inverse ring temp.	**0.78**
El. collision rate	**0.69**
Electron density	**0.55**
Cathode areas inverse ratio	**0.59**

Tab 1: Correlation between etch rate, surface temperature, plasma parameters, and electrode area.

To improve the uniformity of a nitride etch process at a MxP chamber, several shadow rings were tested. They are located around the wafer electrode and behave like a virtual part thereof. While the rf power was kept constant, the etch rate varied, depending on the shadow ring material. Figure 25 shows the bulk power, measured for a two step process with a high permittivity Si shadow ring and a low permittivity quartz shadow ring. The two etch steps can be clearly distinguished. Bulk power and electron collision rate, too, measured with the low permittivity quartz shadow ring installed, are significantly higher. The values of bulk power and electron collision rate correlate with the etch rate and the wafer surface temperature. Because of its capacitive coupling to the wafer electrode, the high permittivity Si ring acts as a rf conducting part of the wafer electrode. As a result, the same rf power is spread on a "larger wafer" with a diameter of 260 mm. All measured parameters correlate well with the calculated inverse area ratio of the rf conducting wafer electrode area (see Tab 1).

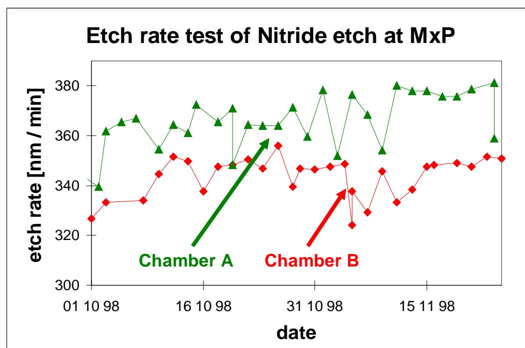

Figure 26: Comparison of nitride etch rate at two Applied Materials MxP chambers

Parameter	Ratio Chamber A / Chamber B
Nitride etch rate	**1,17**
Electron collision rate	**1,19**
Electron density	1,02
Bulk power	**1,21**

Tab 2: Comparison of nitride etch rate with plasma parameters for two chambers.

Tab 2 compares the nitride etch rate at two Applied Materials MxP chambers with the plasma parameters (see also Figure 26). Electron collision rate and bulk power correlate with etch rate, while electron density remains constant.

5.7. Tool failure detection

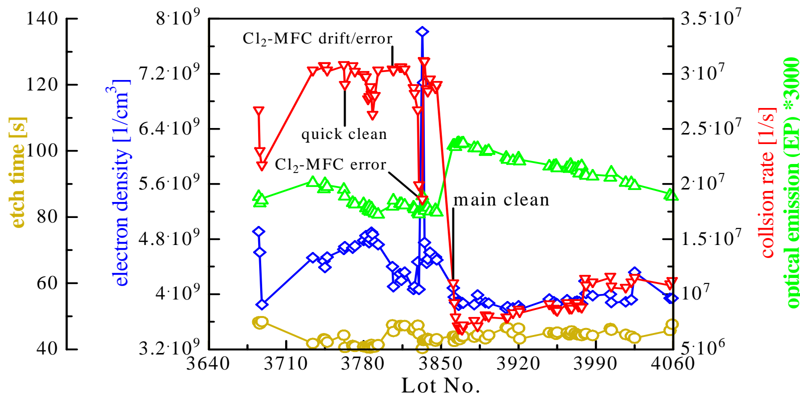

Figure 27: Tool failure detection during Al etch at LAM TCP; one point – mean of one lot

During monitoring of product lots at LAM TCP 9600SE, effects of quick clean and main clean on the chamber were detected [7, 8] (see **Figure 27**). Furthermore, the electron collision rate indicated a Cl MFC failure much earlier, than the tool itself.

Figure 28 shows mean values of bulk power for product lots and test wafers as obtained for oxide etch in a MxP+ chamber, measured during the 5th wet clean cycle. The mean values of bulk power and the standard deviation, increased significantly. The time resolved results indicate plasma instabilities (compare Figure 29). These variations were caused by a parasitic plasma in the helium feedthrough of the wafer back side cooling.

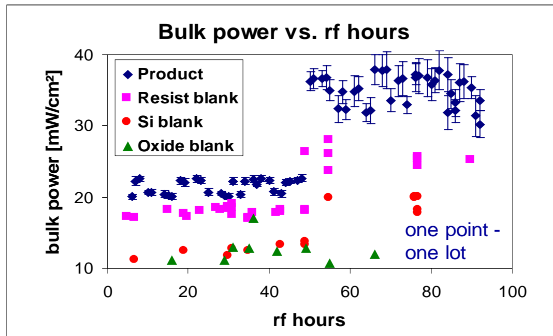

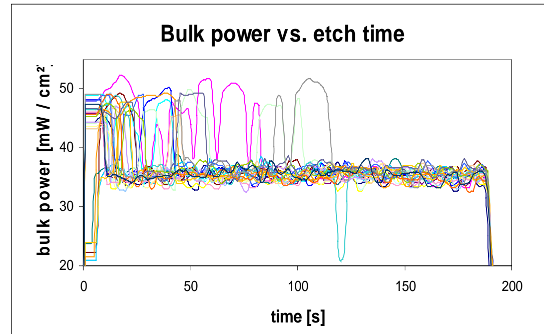

Figure 28: Tool failure detection during oxide etch at Applied Materials MxP+; one point – one lot.

Figure 29: Time depending bulk power indicates plasma instabilities during oxide etch at MxP+ chamber; one curve – one wafer.

5.8. Arcing detection

During conditioning after a wet clean of an Applied Materials MxP+ chamber, a high wafer mean value of the electron collision rate was observed for wafer 9 (see Figure 30). The time resolved curve for the respective process indicates a short and heavy arcing (see Figure 31).

We found hot spots on the electrostatic chuck and at the backside of the wafer. In comparison to all measured tool parameters, e.g. reflected power, bias voltage, and load and tune of the matching network, the electron collision rate was the most sensitive parameter.

Arcing

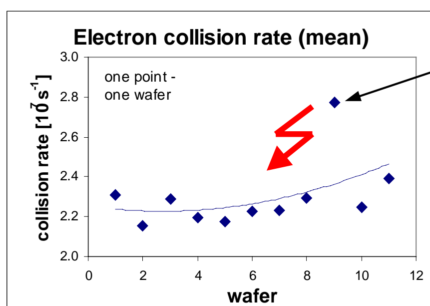

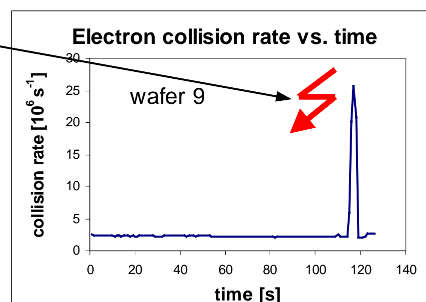

Figure 30: Wafer mean value of electron collision rate measured on wafer 9 indicates arcing.

Figure 31: Time resolved measurement of electron collision rate at wafer 9.

6. SUMMARY

Due to the increasing demands on process control, which are foremost triggered by decreasing feature sizes, increasing integration levels and larger wafer diameters (300 mm) current process controls will have to be supplemented and/or replaced by new in-situ, real time process controls. This transition from **S**tatistical **P**rocess **C**ontrol to **A**dvanced **E**quipment **C**ontrol (AEC) and **A**dvanced **P**rocess **C**ontrol (APC) is already on it's way. Most important for this transition is the availability of production compatible sensors measuring relevant process parameters. The SEERS sensor is a powerful example for the recently developed plasma diagnostic techniques, which can be applied for in – situ, real time process monitoring, and control [18,19]. It can be used for

- Development and optimization of processes
- Measurement of process and tool stability
- Tool matching and base lining
- Measurement of power coupling into plasma
- Improvement of process transfer
- Endpoint detection
- Optimization of chamber cleaning and conditioning
- Detection of process and tool failures, Arcing detection

New plasma measuring techniques are indispensable tools to:
- achieve higher yield
- reduce costs of test wafers and maintenance.

The semiconductor industry has a great potential for reducing costs by integrating process diagnostics like HERCULES into a fab wide sensor / actuator network. However, it has to be clearly seen, that the full potential of these integrated sensors can only be developed if and only if the respective resources, i.e. foremost personnel and infrastructure, are available.

7. REFERENCES

[1] J. D. Austin, *Solid State Technology*, p. 184, September 1997.

[2] S. W. Butler, J. Hosch TI, A. D. Diebold, and B. van Eck, *SemaTech Fab International*, Vol. 1, p. 315.

[3] A. Steinbach, S. Wurm, Ch. Koelbl, D. Köhler, D. Knobloch, and F Bell, " Plasma etch control by means of physical plasma parameters with Hercules" SEMATECH AEC / APC X Symposium on Advanced Equipment Control and Advanced Process Control, 11 – 16 October, Vail / Colorado, USA 1998.

[4] A. Steinbach, S. Wurm, Ch. Koelbl, D. Köhler, D. Knobloch, and F. Bell, "Real time plasma etch control by means of physical plasma parameters with HERCULES", SemiPAC; 24 - 27 January, San Antonio / Texas, USA 1999.

[5] S. Wurm, A. Steinbach, Ch. Koelbl, and F. Bell, Process and Equipment Control for Plasma Etching, Radio Frequency Advisory Group Meeting, September 16-17, San Jose / CA, USA 1998.

[6] A. Steinbach, S. Wurm, S. Bernhard, Ch. Koelbl, M. Sussiek, D. Knobloch,"Real time plasma etch control by means of physical plasma parameters with HERCULES", Proc. of the Workshop on "Low Temperature Plasma Diagnostics III - Diagnostics of Industrial Plasmas", 15 - 19 February 1999, Saillon, Switzerland.

[7] S. Wurm, W. Preis, Ch. Köbl, M. Klick, D. Suchland, M. Kammeyer, and A. Steinmetz, Proceedings. of the Plasma Etch Users Group, 4th Intern. Workshop on Advanced Plasma Tools and Process Engineering, p. 2-7, May 26-27 Millbrae / CA, USA 1998.

[8] S. Wurm, W. Preis, and M. Klick, submitted to *Solid State Technology*, 1998.

[9] R. S. Harp and F. W. Crawford, *J. Appl. Phys*. **35**, 3436 (1964).

[10] M. Klick, *J. Appl. Phys*. **79**, 3445 (1996).

[11] M. Klick and W. Rehak, 12th International Symposium on Plasma Chemistry, Minneapolis, August 1995, University of Minnesota, 1995, Vol. 1 pp. 511-516.

[12] M. Klick, Proceedings of the 10th International Colloquium on Plasma Processes, French Vacuum Society, Antibes, 1995, p. 341.

[13] M. Klick, M. Kammeyer, W. Rehak, W. Kasper, P. Awakowicz, and G. Franz, 5th International Conference on Plasma Surface Engineering, Garmisch-Partenkirchen, Germany 1996.

[14] M. Klick, W. Rehak and M. Kammeyer, *Jpn. J. Appl. Phys*. **36**, 4625 (1997)

[15] M. Klick, Frontiers in Low Temperature Plasma Diagnostics II, Bad Honnef, Germany 1997.

[16] M. A. Lieberman and A. J. Lichtenberg, "Principles of plasma discharges and materials processing" (John Wiley & Sons, New York, 1994), p.355.

[17] V. A. Godyak, R. B. Piejak, and B. M. Alexandrovich, IEE Trans. Plasma Sci. **19** 666 (1991).

[18] M. Derie, "Critical dimension and oxide damage control during Poly/Polycide etching on a TCP 9400SE, using the SEERS plasma diagnostic system.", The European Symposium on Microelectronic Manufacturing Technologies, 19-21 May 1999, Caledonian Hotel, Edinburgh, Scotland, United Kingdom

[19] G. Petit, "Methodololy to improve mean time between clean and decrease defectivity on LAM TCP 9600 by using Self Excited Electron Plasma Resonance Spectroscopy.", The European Symposium on Microelectronic Manufacturing Technologies, 19-21 May 1999, Caledonian Hotel, Edinburgh, Scotland, United Kingdom